AIP Applied Physics Letters

# Repeatable low-temperature negative-differential resistance from Al0.18Ga0.82N/GaN resonant tunneling diodes grown by molecular-beam epitaxy on free-standing GaN substrates

D. Li, L. Tang, C. Edmunds, J. Shao, G. Gardner et al.

Citation: Appl. Phys. Lett. **100**, 252105 (2012); doi: 10.1063/1.4729819

View online: http://dx.doi.org/10.1063/1.4729819

View Table of Contents: http://apl.aip.org/resource/1/APPLAB/v100/i25

Published by the American Institute of Physics.

## Related Articles

Coaxial nanowire resonant tunneling diodes from non-polar AlN/GaN on silicon
Appl. Phys. Lett. 100, 142115 (2012)

A tunnel-induced injection field-effect transistor with steep subthreshold slope and high on-off current ratio
Appl. Phys. Lett. 100, 113512 (2012)

Observation of resonant tunneling phenomenon in metal-insulator-insulator-insulator-metal electron tunnel devices
Appl. Phys. Lett. 100, 113503 (2012)

High 5.2 peak-to-valley current ratio in Si/SiGe resonant interband tunnel diodes grown by chemical vapor deposition
Appl. Phys. Lett. 100, 092104 (2012)

Anisotropic magneto-resistance in a GaMnAs-based single impurity tunnel diode: A tight binding approach
Appl. Phys. Lett. 100, 062403 (2012)

## Additional information on Appl. Phys. Lett.

Journal Homepage: http://apl.aip.org/

Journal Information: http://apl.aip.org/about/about_the_journal

Top downloads: http://apl.aip.org/features/most_downloaded

Information for Authors: http://apl.aip.org/authors

ADVERTISEMENT

Agilent Technologies

Agilent Education and Research Resources DVD 2012

Packed with over 100 NEW articles, application notes, webcasts, and videos relating to Renewable Energy, Nanoscience, RF/Wireless, MIMO, Materials, Digital Signals, Photonics, and General Test & Measurement.

Click Here to Order Your DVD

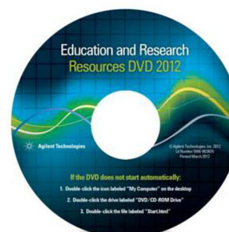

Agilent Technologies

# Repeatable low-temperature negative-differential resistance from $Al_{0.18}Ga_{0.82}N$/GaN resonant tunneling diodes grown by molecular-beam epitaxy on free-standing GaN substrates

D. Li,[1] L. Tang,[1] C. Edmunds,[1] J. Shao,[1] G. Gardner,[2,3] M. J. Manfra,[1,2,3,4] and O. Malis[1,a)]
[1]*Department of Physics, Purdue University, West Lafayette, Indiana 47907, USA*
[2]*Birck Nanotechnology Center, West Lafayette, Indiana 47907, USA*
[3]*School of Materials Engineering, Purdue University, West Lafayette, Indiana 47907, USA*
[4]*School of Electrical and Computer Engineering, Purdue University, West Lafayette, Indiana 47907, USA*

(Received 10 April 2012; accepted 3 June 2012; published online 19 June 2012)

Low-aluminum composition AlGaN/GaN double-barrier resonant tunneling structures were grown by plasma-assisted molecular-beam-epitaxy on free-standing c-plane GaN substrates grown by hydride-vapor phase epitaxy. Clear, exactly reproducible, negative-differential resistance signatures were observed from $4 \times 4\,\mu m^2$ devices at 1.5 V and 1.7 V at 77 K. The relatively small value of the maximum peak-to-valley ratio (1.03) and the area dependence of the electrical characteristics suggest that charge transport is affected by leakage paths through dislocations. However, the reproducibility of the data indicates that electrical traps play no significant role in the charge transport in resonant tunneling diodes grown by molecular-beam-epitaxy under Ga-rich conditions on free-standing GaN substrates. © *2012 American Institute of Physics.*
[http://dx.doi.org/10.1063/1.4729819]

Negative differential resistance (NDR) in double-barrier resonant tunneling diodes (RTDs) is the standard benchmark for vertical charge transport in quantum devices. NDR in RTDs has been demonstrated with several semiconductor material systems (arsenides[1] or the antimonides[2]) but remains challenging for nitride RTDs,[3–17] in spite of the tremendous progress and commercial viability of nitride devices with horizontal electron transport (e.g., high electron mobility transistors)[18] and visible lasers with vertical transport.[19] Resonant tunneling is particularly important for infrared intersubband (ISB) devices such as the quantum cascade lasers (QCLs)[20] and the quantum well infrared photodetectors (QWIPs).[21] Due to unique material properties of GaN/Al(Ga)N heterostructures, such as large conduction band offsets (up to 2.1 eV), large longitudinal-optical phonon energy (90 meV), short lifetimes, and thermal stability, the nitrides are interesting for QCLs in the currently underdeveloped near-infrared (1.5–3 $\mu$m) and far-infrared (25–70 $\mu$m) ranges. Since selective charge injection into the upper laser state of a QCL is achieved through resonant tunneling from the ground state of the injector, demonstration of reliable quantum tunneling in nitride heterostructures is an important step towards realization of nitride QCLs.

The initial papers on nitrides RTDs revealed issues related to the stability and reproducibility of the electrical characteristics.[3–17] To date there have been several reports of NDR in nitride double-barrier structures, but in all cases the I-V characteristics of the RTDs differ drastically from the characteristics of arsenide RTDs. In most reports of c-plane nitride RTDs, the current is found to degrade irreversibly upon repeated voltage ramping, raising the question whether the observed NDR is really due to resonant tunneling through the double barrier. A bi-stable behavior (different I-V depending on the direction of the voltage sweep) was also reported in AlN/GaN RTDs.[15] The degradation of the current has been attributed to filling of traps possibly related to the threading dislocations in nitrides,[3,10] but the physical origin of these traps remains uncertain. Some reproducibility of NDR has been claimed on c-plane GaN substrates under special (negative) pre-biasing conditions,[10] but to date, repeatable electrical characteristics have been reported only on nonpolar nitride RTDs, with either cubic heterostructures[22] or wurtzite nitrides on nonpolar (m-plane) GaN substrates[8] and in nitride nanowires.[9,23] It is noteworthy that the lower effective mass of cubic nitrides would be beneficial for vertical transport devices based on resonant tunneling, but the structural quality of cubic nitrides is still far from matching the quality of wurtzite heterostructures. Sequential tunneling transport in multi-QW structures has also been reported.[24]

In this paper we report repeatable, clear negative-differential resistance signatures appearing at low-temperature from low Al-composition double-barrier AlGaN/GaN heterostructures grown by plasma-assisted molecular-beam epitaxy (MBE) on high-quality free-standing GaN substrates. In order to limit the effects of the dislocations on vertical transport, we have grown RTD structures by MBE on free-standing n++ GaN substrates grown by HVPE (dislocation density $<5 \times 10^6\,cm^{-2}$) supplied by Kyma Technologies, and the device dimensions have been reduced to $4 \times 4\,\mu m^2$. Since relaxation of the heavily-strained AlGaN barrier layers during MBE or subsequent device processing is a major concern for these devices, the Al-composition in the barrier layer was limited to 18%. Since the electric field across a barrier depends not only on applied bias but also on internal polarization field due to polarization discontinuities at interfaces, the low Al-composition in the barrier also limits polarization discontinuities and reduces the possibility of electrical breakdown during operation by reducing built-in electric fields. For this

a)Electronic mail: omalis@purdue.edu.

 © 2012 American Institute of Physics

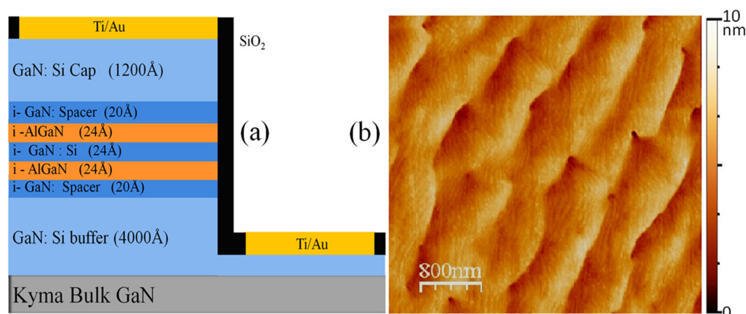


FIG. 1. (a) A schematic view of the designed RTD structure, (b) AFM image of as-grown RTD surface. The $4 \times 4\,\mu m^2$ region has a RMS roughness of 8 Å.

Al-composition, the conduction band offset (0.34 eV) and the intersubband level spacing are similar to standard mid-infrared arsenide QCL materials (i.e., GaAs/AlGaAs and InGaAs/AlInAs), and, therefore, NDR is expected to improve as the temperature is reduced below room temperature, consistent with our findings. Our results are promising for the prospects of vertical transport nitride intersubband devices. In particular, this experimental study is relevant for the use of nitride ISB heterostructures for THz lasers with applications in THz spectroscopy and imaging.

A schematic of the layer thicknesses, doping, and alloy composition of the RTD structures studied in this paper is given in Fig. 1(a). The epitaxial layers were deposited under Ga-rich conditions at 745 °C in a Riber 3200 MBE reactor equipped with a Veeco nitrogen plasma source. A Si-doped, 400 nm-thick buffer layer serves as bottom contact layer. The active region was composed of a $Al_{0.18}Ga_{0.82}N$/GaN/$Al_{0.18}Ga_{0.82}N$ quantum well structure and is sandwiched between undoped 20 Å GaN spacer layers. The whole structure was capped with a 1200 Å GaN layer with silicon doping at a level of $1 \times 10^{19}\,cm^{-3}$ that also serves as the top contact layer. A typical atomic force microscope (AFM) image taken from the as-grown RTD surface is shown in Fig. 1(b). The $4 \times 4\,\mu m^2$ region has a root-mean-square (RMS) roughness of 8 Å.

The RTD device geometry was chosen to have a standard mesa structure optimized for minimal back contact resistance. Device fabrication was performed through standard nitride processing technologies. Mesas were defined using UV lithography and inductively coupled plasma reactive ion etching (ICP-RIE) with $Cl_2$ gas. Then, 3000 Å of $SiO_2$ was deposited by plasma-enhanced chemical vapor deposition (PECVD), and windows were opened for the top and bottom contacts by $CF_4$+$O_2$ plasma etching. Finally, contact layers of Ti/Au with thicknesses of 50 nm/200 nm were deposited by e-beam evaporation. The specific contact resistivity of the back contact measured by the transmission line method is about $6 \times 10^{-5}\,\Omega cm^2$. A top-view scanning electron microscope (SEM) image of a fabricated RTD with mesa size $4 \times 4\,\mu m^2$ is shown in Fig. 2. No devices with area smaller than $4 \times 4\,\mu m^2$ could be fabricated reliably with optical lithography.

The semiconductor chips were mounted on Cu heat sinks and wire-bonded to Au pads. The temperature-dependent current-voltage (I-V) characteristics were measured in a liquid nitrogen-flow cryostat. The positive polarity refers to positive bias applied to the top of the mesa. I-V curves were recorded using an HP4145B semiconductor parameter analyzer that was set up to output a voltage sweep (V) while measuring current (I). Fig. 3(a) shows I-V scans of a typical RTD with mesa size $4 \times 4\,\mu m^2$ taken by sweeping the voltage from 1.3 V to 1.8 V while recording current through the mesa. Small but clear NDR signatures were observed around 1.5 V and 1.7 V at 77 K with peak current density of 122 kA/cm$^2$. Importantly, the I-Vs are identical on the voltage ramp-up and ramp-down. No significant degradation of the device performance was observed after 20 I-V measurements, in contrast to most previous reports on c-plane GaN.[3,7,8,10] The peak-to-valley ratio (PVR) remains the same after 20 measurements, but the position of the resonances appears to shift to slightly higher voltages after reverse bias to −3 V (shown in Fig. 3(b)). This shift of about 0.05 V may be related to charge redistribution along interfaces, possibly even to charge trapping on defects. However, this effect is negligible when compared to the bistable behavior reported earlier (see for example Ref. 15). Fig. 3(b) gives a typical I-V curve under reverse bias scanned from 0 V to −2 V. A small feature is also visible in reverse bias around −0.75 V. We note that at least one NDR feature is expected in reverse bias, but the reverse current is expected to be smaller due to an effectively thicker potential barrier. The I-V characteristics do not change significantly if the temperature is lowered to 4 K, and the two NDR features are distinguishable up to 110 K. It is also noteworthy that we observed NDR in several small size ($4 \times 4\,\mu m^2$) devices from two different wafers. No NDR features, however, were observed from any larger area devices ($6 \times 6\,\mu m^2$ to $30 \times 30\,\mu m^2$).

Fig. 4 shows the schematics of the conduction band diagram in the active region of our RTDs at zero bias as

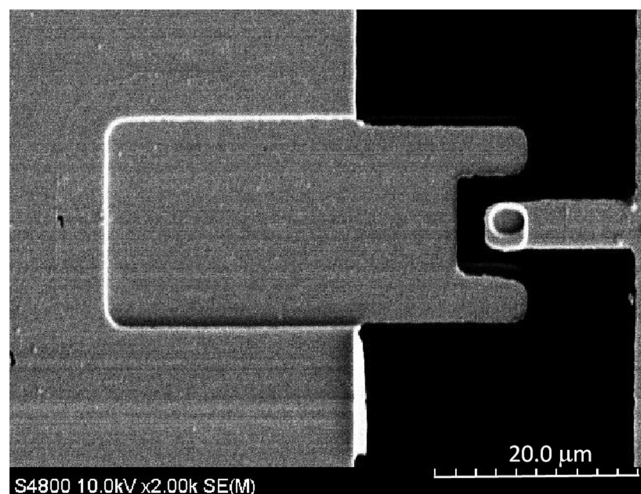


FIG. 2. Top-view SEM image of the fabricated $4 \times 4\,\mu m^2$ RTD device showing the $2 \times 2\,\mu m^2$ window opened on the mesa for the top contact, and the mesa surrounded by the bottom contact.

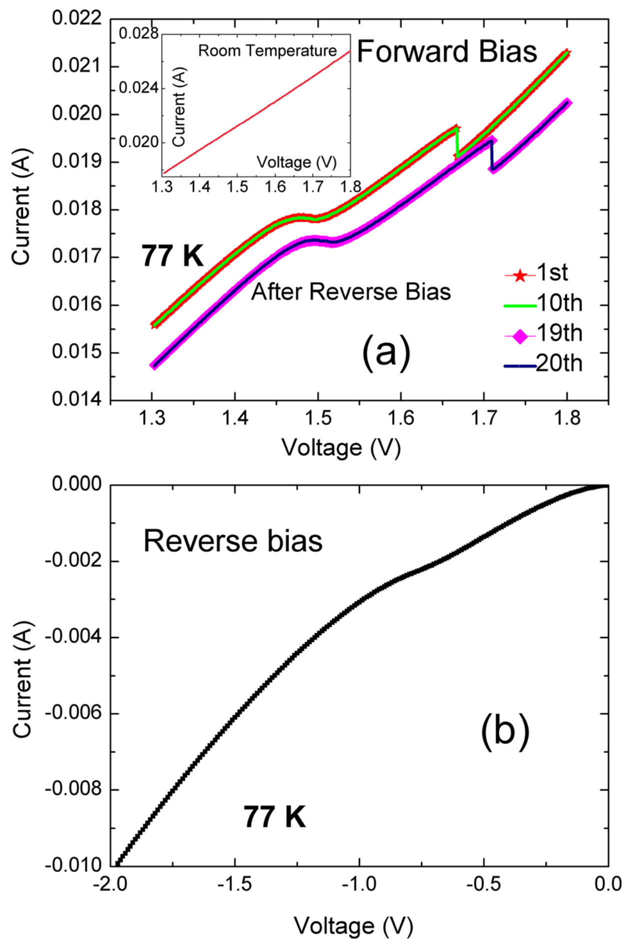


FIG. 3. I-V characteristics of an RTD at 77 K by sweeping the bias on the mesa top while recording current through mesa. (a) Voltage was scanned from 1.3 V to 1.8 V for 20 times and the data is shown for the 1st, 10th, 19th, and 20th measurements. Note that the I-Vs are identical on the voltage ramp-up and ramp-down. The device was reversely biased after the 18th measurement as shown in (b). The inset of (a) shows the room temperature I-V curve for the same device. (b) I-V for reverse bias scanned from 0 V to −2 V applied to the same device.

calculated with the self-consistent Schroedinger/Poisson solver nextnano3.[25] The double-barrier structure exhibits two quantized states at $E_1 = 0.204$ eV and $E_2 = 0.480$ eV.

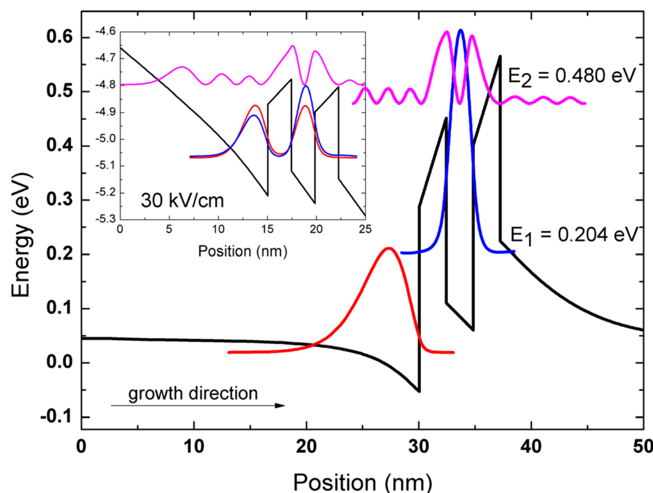


FIG. 4. Schematic conduction band diagram of the active region at zero bias. The eigenvalues of the confined wave functions in the quantum well are $E_1 = 0.204$ eV and $E_2 = 0.480$ eV at 77 K. The inset shows the structure under a uniform field of 30 kV/cm.

The observed resonant tunneling voltages ($V_{NDR}$) in our devices were higher than expected, possibly due to series contact resistance. However, the resonances were observed at considerably lower voltages than reported in other papers (up to 4 V),[8–10] a fact that indicates a higher quality of the electrical contacts. Most relevant, the voltage difference between the two observed NDR features is consistent with the energy difference between the quantized calculated energies (∼0.2 eV). The simulations of the structure under bias show that resonant tunneling occurs from the lowest quantum level in the triangular well on the left to the quantum state in the well, and then to the continuum (inset of Fig. 4). Due to the close spacing of the levels in the triangular well at low bias, tunneling into the lowest quantized state should be broadened and as a result the NDR signature should be weak, consistent with our data. At higher bias the quantized levels in the triangular well become better separated and hence the NDR feature is expected to get sharper. However, it is also noteworthy that the $E_2$ resonance is weakly confined (quasi-bound state) and strongly dependent on the exact Al-composition of the barriers. Under higher bias, resonant tunneling occurs from the lowest level of the triangular well directly into this quasi-bound state across a single AlGaN barrier (the second barrier is below $E_2$). This may be the reason why the PVR observed for $E_2$ is still low, but higher than for $E_1$.

In summary, we report the observation of reproducible NDR signatures at 77 K from low Al-composition AlGaN/GaN double-barrier RTDs grown by MBE on n++ free-standing GaN substrates. The PVR (1.03) of the NDR did not degrade significantly after 20 I-V scans and was found to be comparable with the PVR reported for defect-free single GaN quantum disks in double-barrier AlN/GaN nanowires (1.05 at 77 K).[23] However, the NDR was visible only in the small area devices ($4 \times 4\,\mu m^2$). Based on our previous studies of transport through dislocations in AlGaN/GaN heterostructures,[26,27] we attribute the area sensitivity of the I-V curves to leakage conduction through screw (conductive) dislocations. This leakage path is likely dominating transport for larger area devices obscuring any NDR features, but plays a smaller role for the small area devices. The leakage current appears to increase linearly with the mesa area for the smaller area devices ($4 \times 4\,\mu m^2$, $6 \times 6\,\mu m^2$, and $8 \times 8\,\mu m^2$), but sub-linearly when larger area devices are considered ($30 \times 30\,\mu m^2$). The latter is likely due to the non-uniform distribution of conductive defects on the surface. Therefore, further improvements of epilayer growth, optimization of the device layer structure, and further substrate defect reduction are essential for increasing the PVR of future nitride RTDs and achieving room-temperature operation. From a material standpoint, our results indicate that traps do not play a significant role in the charge transport in RTDs grown by MBE under Ga-rich conditions on free-standing GaN substrates grown by HVPE. Our results are encouraging for the prospects of nitride quantum cascade lasers, especially for the far-infrared (terahertz) range.

This work was supported by the NSF Award No. ECCS-1001431 and from the Defense Advanced Research Project Agency (DARPA) under Contract No. D11PC20027.

[1]L. L. Chang, L. Esaki, and R. Tsu, Appl. Phys. Lett. **24**, 593 (1974).
[2]E. R. Brown, T. C. L. G. Sollner, C. D. Parker, W. D. Goodhue, and C. L. Chen, Appl. Phys. Lett. **55**, 1777 (1989).
[3]S. Golka, C. Pflugl, W. Schrenk, G. Strasser, C. Skierbiszewski, M. Siekacz, I. Grzegory, and S. Porowski, Appl. Phys. Lett. **88**, 172106 (2006).
[4]E. Baumann, F. R. Giorgetta, D. Hofstetter, H. Wu, W. J. Schaff, L. F. Eastman, and L. Kirste, Appl. Phys. Lett. **86**, 032110 (2005).
[5]A. E. Belyaev, C. T. Foxon, S. V. Novikov, O. Makarovsky, L. Eaves, M. J. Kappers, and C. J. Humphreys, Appl. Phys. Lett. **83**, 3626 (2003).
[6]C. Bayram, Z. Vashaei, and M. Razeghi, Appl. Phys. Lett. **96**, 042103 (2010).
[7]Z. Vashaei, C. Bayram, and M. Razeghi, J. Appl. Phys. **107**, 083505 (2010).
[8]C. Bayram, Z. Vashaei, and M. Razeghi, Appl. Phys. Lett. **97**, 181109 (2010).
[9]R. Songmuang, G. Katsaros, E. Monroy, P. Spathis, C. Bougerol, M. Mongillo, and S. De Franceschi, Nano Lett. **10**, 3545 (2010).
[10]M. Boucherit, A. Soltani, E. Monroy, M. Rousseau, D. Deresmes, M. Berthe, C. Durand, and J.-C. De Jaeger, Appl. Phys. Lett. **99**, 182109 (2011).
[11]A. Kikuchi, R. Bannai, K. Kishino, C.-M. Lee, and J.-I. Chyi, Appl. Phys. Lett. **81**, 1729 (2002).
[12]C. T. Foxon, S. V. Novikov, A. E. Belyaev, L. X. Zhao, O. Makarovsky, D. J. Walker, L. Eaves, R. I. Dykeman, S. V. Danylyuk, S. A. Vitusevich, M. J. Kappers, J. S. Barnard, and C. J. Humphreys, Phys. Status Solidi C **0**, 2389 (2003).
[13]A. E. Belyaev, O. Makarovsky, D. J. Walker, L. Eaves, C. T. Foxon, S. V. Novikov, L. X. Zhao, R. I. Dykeman, S. V. Danylyuk, S. A. Vitusevich, M. J. Kappers, J. S. Barnard, and C. J. Humphreys, Physica E **21**, 752 (2004).
[14]S. Golka, G. Pozzovivo, W. Schrenk, G. Strasser, C. Skierbiszewski, M. Siekacz, I. Grzegory, and S. Porowski, AIP Conf. Proc. **893**, 303 (2007).
[15]S. Leconte, S. Golka, G. Pozzovivo, G. Strasser, T. Remmele, M. Albrecht, and E. Monroy, Phys. Status Solidi C – Curr. Top. Solid State Phys. **5**(2), 431 (2008).
[16]C. Bayram, Z. Vashaei, and M. Razeghi, Appl. Phys. Lett. **97**, 092104 (2010).
[17]Z. Vashaei, C. Bayram, R. McClintock, and M. Razeghi, in Proceedings of the Conference on Quantum Sensing and Nanophotonic Devices VIII, San Francisco, CA, 24 January 2011.
[18]Y. Wu, A. Saxler, M. Moore, R. P. Smith, S. Sheppard, P. M. Chavarkar, T. Wisleder, U. K. Mishra, and P. Parikh, IEEE Electron Device Lett. **25**, 117 (2004).
[19]S. Nakamura, M. Senoh, S. Nagahama, N. Iwasa, T. Yamada, T. Matsushita, Y. Sugimoto, and H. Kiyoku, Appl. Phys. Lett. **69**, 1477 (1996).
[20]C. Gmachl, F. Capasso, D. L. Sivco, and A. Y. Cho, Rep. Prog. Phys. **64**, 1533 (2001).
[21]E. Baumann, F. R. Giorgetta, D. Hofstetter, H. Lu, X. Chen, W. J. Scha, L. F. Eastman, S. Golka, W. Schrenk, and G. Strasser, Appl. Phys. Lett. **87**, 191102 (2005).
[22]N. Zainal, S. V. Novikov, C. J. Mellor, C. T. Foxon, and A. J. Kent, Appl. Phys. Lett. **97**, 112102 (2010).
[23]L. Rigutti, G. Jacopin, A. D. Bugallo, M. Tchernycheva, E. Warde, F. H. Julien, R. Songmuang, E. Galopin, L. Largeau, and J. C. Harmand, Nanotechnology **21**, 425206 (2010).
[24]F. Sudradjat, W. Zhang, K. Driscoll, Y. T. Liao, A. Bhattacharyya, C. Thomidis, L. Zhou, D. J. Smith, T. D. Moustakas, and R. Paiella, J. Appl. Phys. **108**, 103704 (2010).
[25]S. Birner, T. Zibold, T. Andlauer, T. Kubis, M. Sabathil, A. Trellakis, and P. Vogl, IEEE Trans. Electron Devices **54**, 2137 (2007).
[26]J. W. P. Hsu, M. J. Manfra, R. J. Molnar, B. Heying, and J. S. Speck, Appl. Phys. Lett. **81**, 79 (2002).
[27]J. W. P. Hsu, M. J. Manfra, D. V. Lang, S. Richter, and S. N. G. Chu, Appl. Phys. Lett. **78**, 1685, 2001.